REVISITING THE LYC ESCAPE FRACTION CRISIS: PREDICTIONS FOR $Z > 6$ FROM LOCALS

Andreas L. Faisst

Infrared Processing and Analysis Center, California Institute of Technology, Pasadena, CA 91125, USA

ABSTRACT

The intrinsic escape fraction of ionizing Lyman continuum photons (f_{esc}) is crucial to understand whether galaxies are capable of reionizing the neutral hydrogen in the early universe at $z > 6$. Unfortunately, it is not possible to access f_{esc} at $z > 4$ with direct observations and the handful of measurements from low redshift galaxies consistently find $f_{esc} < 10\%$, while at least $f_{esc} \sim 10\%$ is necessary for galaxies dominate reionization. Here, we present the first empirical prediction of f_{esc} at $z > 6$ by combining the (sparsely populated) relation between [O III]/[O II] and f_{esc} with the redshift evolution of [O III]/[O II] as predicted from local high-z analogs selected by their Hα equivalent-width. We find $f_{esc} = 5.7^{+8.3}_{-3.3}\%$ at $z = 6$ and $f_{esc} = 10.4^{+15.5}_{-6.3}\%$ at $z = 9$ for galaxies with $\log(M/M_\odot) \sim 9.0$ (errors given as 1σ). However, there is a negative correlation with stellar mass and we find up to 50% larger f_{esc} per 0.5 dex decrease in stellar mass. The population averaged escape fraction increases according to $f_{esc} = f_{esc,0}((1+z)/3)^\alpha$, with $f_{esc,0} = 2.3 \pm 0.05$ and $\alpha = 1.17 \pm 0.02$ at $z > 2$ for $\log(M/M_\odot) \sim 9.0$. With our empirical prediction of f_{esc} (thus fixing an important previously unknown variable) and further reasonable assumption on clumping factor and the production efficiency of Lyman continuum photons, we conclude that the average population of galaxies is just capable to reionize the universe by $z \sim 6$.

Keywords: galaxies: evolution − galaxies: high-redshift − galaxies: ISM

1. INTRODUCTION

A major phase transition in the early universe takes place during the *Epoch of Reionization* (EoR), in which hydrogen in the inter-galactic medium (IGM) is transformed from a neutral to an ionized state. The EoR is closely connected to the formation of the first galaxies and thus the study of its evolution in time and space is important to understand galaxy formation in the early universe.

The study of absorption due to intervening neutral hydrogen in the IGM in ultra-violet (UV) spectra of quasars allow us to pinpoint the end of the EoR (i.e., the time when the universe is fully ionized) to $z \sim 6$ (Fan et al. 2006; McGreer et al. 2011; Mortlock et al. 2011). Furthermore, the rapid decrease in the fraction of star-forming high redshift galaxies with Lyα emission at $z > 6$ suggest that the universe got ionized very quickly on timescales of only a couple 100 Myrs between $z \sim 6 − 10$ (e.g., Stark et al. 2010; Ono et al. 2012; Schenker et al. 2013; Matthee et al. 2014; Faisst et al. 2014; Robertson et al. 2015). In addition to these direct observations, the temperature fluctuations in the cosmic microwave background (CMB) allow the measurement of the integrated density of free electrons from $z = 0$, through the EoR, to $z \sim 1100$ when the CMB emerged. Recent measurements suggest $\tau_e = 0.055 \pm 0.009$ and constrain the end of the EoR to $7.8 \lesssim z_{ion} \lesssim 8.8$ assuming an immediate ionization of hydrogen (Planck Collaboration et al. 2016).

Although such observations are able to reveal the time frame of the EoR, we are mostly tripping in the dark about the origin of the dominant ionizing sources. Quasars and star-forming galaxies are currently the competing players for providing energetic photons to ionize hydrogen at $z > 6$. However, because of the suggested sharp decline in the number density of quasars with increasing redshift at $z > 6$, they likely do not dominate the budget of radiation needed to ionize hydrogen[1] (e.g., Masters et al. 2012; Palanque-Delabrouille et al. 2013). On the other hand, the overall number density of UV emitting, faint star-forming galaxies has only slightly dropped between $6 < z < 9$ (Tacchella et al. 2013; Schenker et al. 2013; Oesch et al. 2014; Bouwens et al. 2015c; Mason et al. 2015). Furthermore, studies

afaisst@ipac.caltech.edu; Twitter: @astrofaisst

[1] However, they contribute to the reionization of Helium at $z \sim 3$ (see also Madau & Haardt 2015).

of faint, lensed galaxies show the continuation of the UV luminosity function (LF) to very faint magnitudes (Alavi et al. 2014; Livermore et al. 2016), thus providing an important number of galaxies needed for reionization.

The redshift evolution of the volume fraction of ionized hydrogen (Q_{HII}) and the integral of the electron scattering optical depth ($\tau_{\mathrm{el}}(z)$, the integrated density of free electrons to redshift z) allow us to test whether galaxies are actually capable of reionizing the universe (e.g., Finkelstein et al. 2012; Kuhlen & Faucher-Giguère 2012; Bouwens et al. 2015a; Robertson et al. 2015; Price et al. 2016). Unfortunately, the determination of $Q_{\mathrm{HII}}(z)$ and $\tau_{\mathrm{el}}(z)$ involves several properties of galaxies and their environment, which cannot be measured directly or have to be accessed via cosmological simulations. In detail, these dependencies are the faint end slope of the UV LF and its cut-off magnitude ($M_{\mathrm{UV,lim}}$), the clumping of hydrogen in the IGM (C), the Lyman continuum (LyC) photon production efficiency (ξ_{ion}), and the intrinsic escape fraction of ionizing LyC photons (f_{esc}). We have a good handle on $M_{\mathrm{UV,lim}}$ from lensing (see above), have a reliable measurement of ξ_{ion} at $z \sim 5$ (e.g., Bouwens et al. 2015b), and can provide a reasonable range in C from cosmological simulations (e.g., Finlator et al. 2012). In contrast, f_{esc} is puzzling and unfortunately directly affecting Q_{HII} and τ_{el} and therefore our picture of galaxies during reionization.

With only f_{esc} as free parameter, different studies suggest that $f_{\mathrm{esc}} = 10\% - 20\%$ at $z > 6$ is necessary for galaxies to fully ionize the universe (Bolton & Haehnelt 2007b; Finkelstein et al. 2012; Kuhlen & Faucher-Giguère 2012; Robertson et al. 2015; Bouwens et al. 2015a,b; Mitra et al. 2015; Price et al. 2016). Simulations do not agree on f_{esc} at high redshifts and find either very high (e.g., Sharma et al. 2016) or very low values (e.g., Gnedin et al. 2008; Ma et al. 2015). Furthermore, they predict a strong dependence on dark matter halo mass and star formation (e.g., Wise & Cen 2009; Razoumov & Sommer-Larsen 2010). Direct observational constraints on f_{esc} in the EoR are not possible because of the increasing opacity of the IGM to LyC photons at $z > 4$ (e.g., Madau 1995; Inoue et al. 2014). Except one possible strong LyC emitter at $z = 3.2$ with $f_{\mathrm{esc}} > 50\%$ (Vanzella et al. 2016), the handful of confirmed LyC emitters at $z < 3$ show all consistently $f_{\mathrm{esc}} \lesssim 8\%$ (Steidel et al. 2001; Leitet et al. 2013; Borthakur et al. 2014; Cooke et al. 2014; Siana et al. 2015; de Barros et al. 2016; Izotov et al. 2016a,b; Smith et al. 2016; Vanzella et al. 2016; Leitherer et al. 2016). The numerous non-detections listed in the literature show upper limits of $f_{\mathrm{esc}} \sim 2\% - 5\%$ over large redshift ranges (Sandberg et al. 2015; Grazian et al. 2016; Rutkowski et al. 2016; Guaita et al. 2016; Vasei et al. 2016). If galaxies are responsible for ionizing the uni-

verse at $z > 6$, clearly, their population averaged LyC escape fraction needs to increase substantially with redshift by at least a factor of two (see also Inoue et al. 2006). *What methods can we use to access f_{esc} observationally in the EoR?* Radiative transfer models suggest a correlation between the ratio of [O III]/[O II] and f_{esc} in density bound H II regions (e.g., Nakajima & Ouchi 2014) and a handful of recent observational studies verify this positive correlation (de Barros et al. 2016; Vanzella et al. 2016; Izotov et al. 2016a,b). The increased [O III]/Hβ ratios found in $z > 5$ galaxies (e.g., Stanway et al. 2014; Roberts-Borsani et al. 2015; Faisst et al. 2016a) hint towards an increasing [O III]/[O II] ratio for the global population of galaxies at high redshifts and therefore could be the smoking gun for a strong evolution in $f_{\mathrm{esc}}(z)$. Currently, the [O II] line cannot be measured spectroscopically at $z > 4$ and the use of broad-band photometry to determine [O II] line strengths is degenerated with the 4000 Å Balmer break, a strong function of age and other galaxy parameters. However, local analogs of high redshift galaxies can be used to probe the physical properties of these galaxies.

This paper aims to provide the first observationally based prediction of f_{esc} in galaxies at $z > 6$. For this to end, we select local high-z analogs (LHAs) by their Hα emission (see Faisst et al. 2016a) to predict the [O III]/[O II] ratios of high redshift galaxies, and, with an empirical correlation between [O III]/[O II] and f_{esc}, ultimately the redshift evolution of f_{esc} (Section 2). With our prediction of f_{esc} we then derive $Q_{\mathrm{HII}}(z)$ and $\tau_{\mathrm{el}}(z)$ and comment on the capability of galaxies to reionize the early universe (Section 3). Throughout this work we adopt a flat cosmology with $\Omega_{\Lambda,0} = 0.7$, $\Omega_{m,0} = 0.3$, and $h = 0.7$. All stellar masses are scaled to a Chabrier (2003) initial mass function.

2. PREDICTING f_{esc} AT HIGH REDSHIFTS

2.1. *Locals as analogs for high redshift galaxies*

The resemblance of the physical properties of high redshift galaxies and sub-sets of galaxies at low ($z < 1$) or local ($z \sim 0$) redshifts has been known since almost a decade and it is subject of study in the very recent literature (Cardamone et al. 2009; Stanway et al. 2014; Greis et al. 2016; Bian et al. 2016; Faisst et al. 2016a; Masters et al. 2016; Erb et al. 2016). Some of the most famous representatives of low redshift high-z analogs are the "Green Peas" at $z \sim 0.2$ (Cardamone et al. 2009) or the ultra strong emission line galaxies at $z \sim 0.8$ (USELs, Hu et al. 2009). In any case, the LHAs are characterized by an increased star-formation rate (SFR)
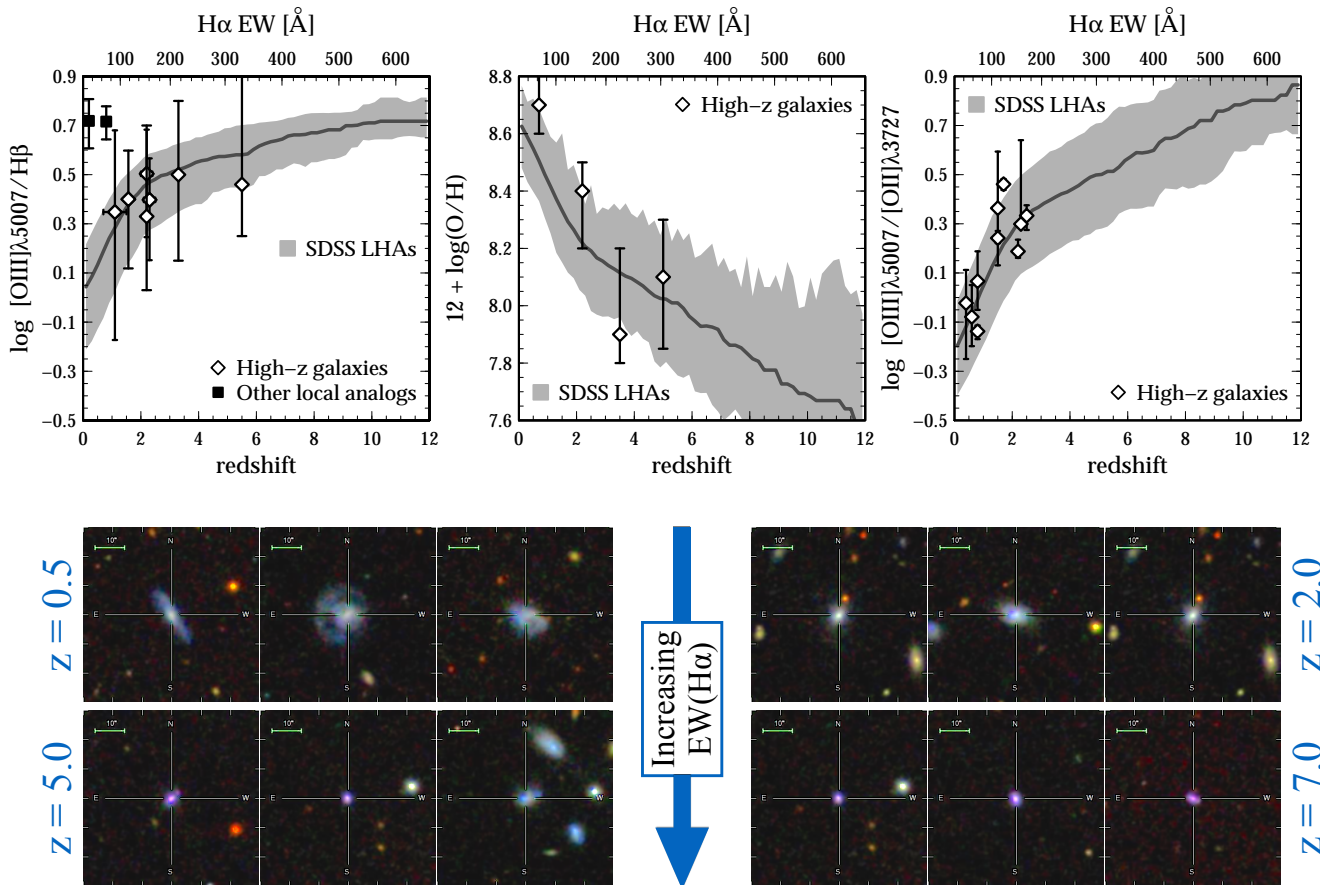
Figure 1. **Top:** The predicted redshift evolution of [O III]/Hβ (left), metallicity (middle), and [O III]/[O II] (right) from Hα EW selected LHAs in SDSS. The symbols show actual measurements from the literature (see text for references) and show a good agreement with the measurement on the LHAs. **Bottom:** SDSS color composites of three randomly picked representatives of LHAs for four different Hα EWs mimicking four different redshifts ($z = 0.5, 2.0, 5.0, 7.0$ from left to right, top to bottom, stamps are $60'' \times 60''$ in size). The LHAs show agreement in morphology with observed high redshift galaxies.

surface density and Hα equivalent-width (EW)[2] compared to the average local galaxy population (Masters et al. 2016). In particular, Faisst et al. (2016a) measure the [O III]/Hβ line ratios of average $z \sim 5.5$ galaxies via the Spitzer color excess and verify a good agreement with LHAs selected by EW(Hα) $> 300\,\text{Å}$. This first-order verification motivates the use of Hα EW selected LHAs to predict spectroscopic properties of high redshift galaxies in the EoR. Here, we use a sample of more than $100,000$ local ($z < 0.1$) galaxies drawn from the Sloan Digital Sky Survey (SDSS, York et al. 2000) DR12 release (Alam et al. 2015) using the SDSS query tool[3]. The galaxies are selected to have S/N > 5 in all the important optical emission lines ([O II], [O III], Hα, Hβ, and [N II]), and no AGN component. We select LHAs for

galaxies at a redshift z by selecting SDSS galaxies with EW(Hα)$|_\text{SDSS}$ = EW(Hα)$(z) \pm \Delta(z)$, using the relation EW(Hα)(z) presented in Faisst et al. (2016a) including the 1σ confidence interval (Δ) in EW at a given z.

We stress that, albeit the obvious similarities of LHAs and intermediate galaxies ($z \sim 2$), the use of LHAs to infer the properties of very high redshift galaxies has not been fully verified, yet. The following results therefore strongly depend on the assumption that strong Hα emitting local galaxies (equivalent to high specific SFR) are indeed similar to actual high-z galaxies and that the ISM properties do not greatly depend on the environment a galaxy was formed in. This has not to be the case, since the cradles of formation for very high-z galaxies surely are different (more dense, more galaxy interactions) compared to the ones of local galaxies. Ultimately, the *James Webb Space Telescope* (JWST) will be able to test these assumptions further and will provide a more clear picture.

2.2. Predicted emission line ratios of high-z galaxies

---

[2] Note that EW(Hα) is proportional to the specific SFR of a galaxy.

[3] http://skyserver.sdss.org/dr12/en/tools/search/sql.aspx

The top panels of Figure 1 show the dependence of spectroscopic galaxy properties on EW(Hα), i.e., the predicted properties of galaxies at redshifts z. We show galaxies with $8.5 < \log(M/M_\odot) < 9.5$ with a median of $\log(M/M_\odot) \sim 9.0$ (similar to the galaxies observed at high redshift) and we will discuss the stellar mass dependence in Section 2.4. We show the redshift evolution of the [O III]/Hβ ratio (left), gas phase metallicity[4] (middle), and [O III]/[O II] ratio (right) inferred from our Hα EW selected SDSS LHAs. The median is shown as black line and the 1σ scatter is visualized by the gray band. The open symbols show the measurement of the three quantities for actual galaxies at high redshift (from either spectroscopy or Spitzer color excess at $z > 4$) from the literature (for [O III]/Hβ: Colbert et al. (2013); Steidel et al. (2014); Sanders et al. (2016); Silverman et al. (2015); for metallicity: Maiolino et al. (2008); Faisst et al. (2016b); for [O III]/[O II]: Rigby et al. (2011); Le Fèvre et al. (2013); de los Reyes et al. (2015); Hayashi et al. (2015); Khostovan et al. (2016)). We also show the properties of other low redshift analogs (Green Peas at $z \sim 0.3$ (Cardamone et al. 2009) and USELs at $z \sim 0.8$ (Hu et al. 2009)) with filled symbols for comparison. All in all, there is a good agreement in all the shown spectral properties of galaxies at high redshift and LHAs purely selected by EW(Hα). This suggests that the Hα EW (closely related to the specific SFR) is strongly correlated with the conditions of the ISM in these galaxies, or, vice versa, the ISM of galaxies with strong Hα emission is very similar at all redshifts up to $z \sim 5$. Under these considerations and with these assumptions, we use the Hα EW as the quantity for the selection of local galaxies to predict the spectral properties of galaxies at $z > 5$ where currently no such measurements are possible.

From the LHAs we infer *average* [O III]/Hβ ratios of $\sim 4-5$ and [O III]/[O II] ratios larger than $3-4$ at $z > 6$. The gas-phase metallicities of $z > 6$ galaxies are predicted to be $12 + \log(O/H) < 8.0$ on average, but with a substantial scatter leading to values of above 8.0 for some galaxies. Such large scatter is consistent with measurements of metallicity in $z \sim 5$ galaxies based on rest-UV absorption features and is expected from the different evolutionary stages and dust attenuation as well as gas inflows in these systems (e.g., Faisst et al. 2016b).

Finally, the bottom panels of Figure 1 show the morphological resemblance of our LHAs with high redshift galaxies. With increasing EW(Hα) (and therefore corresponding redshift), the LHAs become more compact and blue and show clumps in UV light as it is seen in high redshift galaxies at $z = 2-4$ (e.g., Förster Schreiber
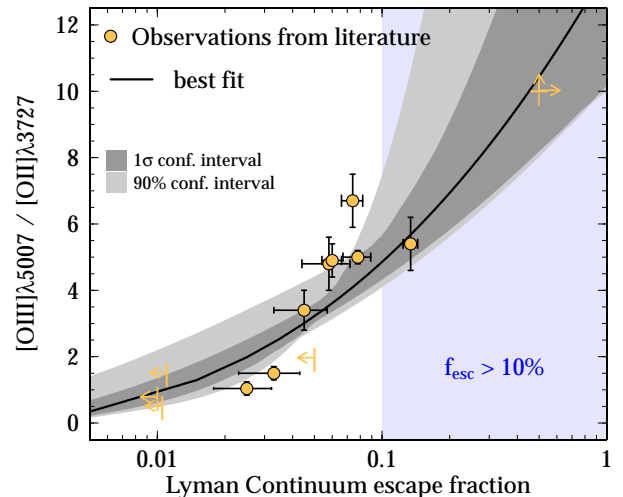

Figure 2. Observed correlation between [O III]/[O II] ratio with f_{esc} from a compilation of literature data with limits shown by arrows. The black line shows the best fit median relation with 1σ and 90% confidence interval envelope. The analytical parametrization is given in Equation 1. The blue shaded area shows $f_{esc} > 10\%$, needed for galaxies at $z > 6$ to reionize the universe.

et al. 2011; Hemmati et al. 2015).

2.3. *Correlation between [O III]/[O II] and f_{esc}*

The absorption of Lyman continuum photons in the IGM increases quickly by a factor of 100 or more close to $z \sim 4$ (e.g., Inoue et al. 2014). The direct measurement of the galaxy intrinsic f_{esc} at redshift greater than this is therefore not possible. However, its theoretically and observationally motivated connection with the [O III]/[O II] ratio may allow us to make predictions of f_{esc} for distant galaxies.

Commonly, f_{esc} is measured in local galaxies from spectra or at intermediate redshifts by the detection of excess flux in narrow-band filters at rest-frame $\lambda < 900\,Å$. As summarized in Section 1, the detection of Lyman continuum photons turns out to be difficult and current searches are mostly ending in non-detections. With the recent addition of Lyman continuum detections in mostly local galaxies, the positive correlation between f_{esc} and the [O III]/[O II] ratio became observationally clear. The [O III]/[O II] ratio is a measure of the ionization parameter in galaxies, which correlates with the star-formation density and thus production of UV photons. A positive correlation is expected from radiative transfer simulations and is physically motivated by density-bound H II regions and stronger radiation fields prevailing in high redshift galaxies. In such environments, an increase in [O III] flux, at a roughly constant [O II] emission, is expected in connection with a large amount of escaping ionizing photons and therefore high f_{esc} (e.g., Nakajima & Ouchi 2014). In Figure 2, we show
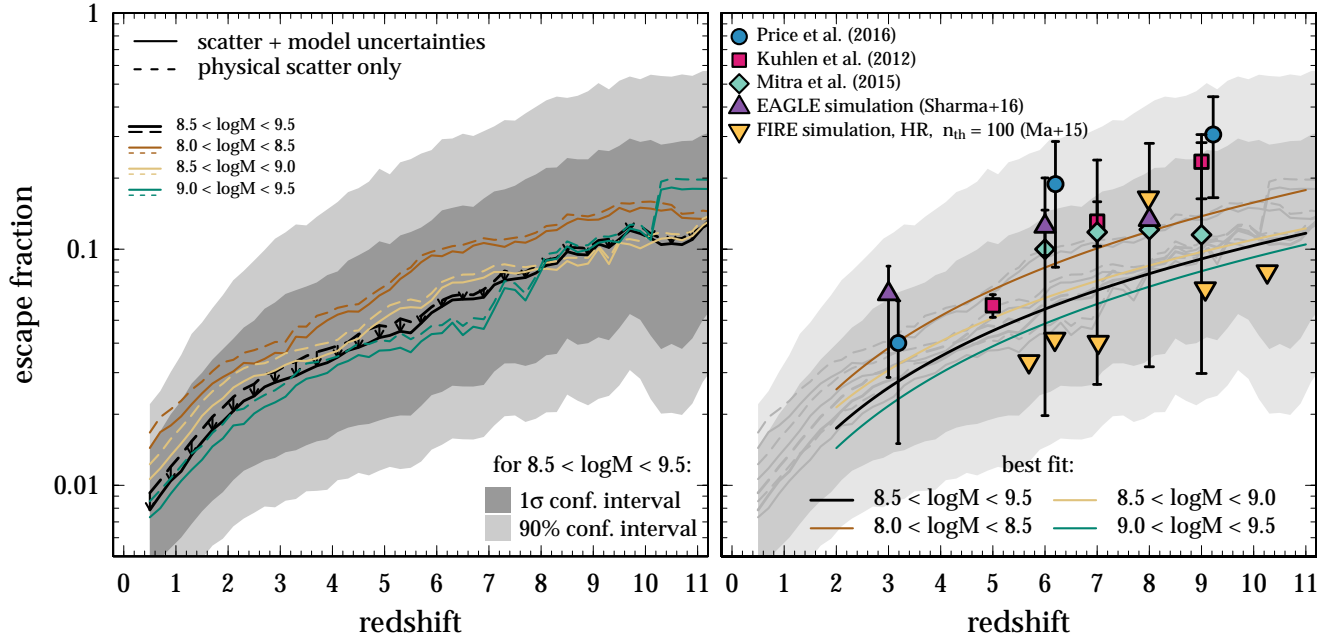
Figure 3. The redshift evolution of f_{esc} infered by our LHAs. **Left:** The thick, black solid line shows the prediction for galaxies with $8.5 < \log(M/M_\odot) < 9.5$ together with 1σ (dark gray) and 90% (light gray) confidence intervals including observed physical scatter in the [O III]/[O II] vs. redshift relation and uncertainties in the [O III]/[O II] vs. f_{esc} fit. The dashed black line, shows the prediction *only* including observational scatter (assuming no uncertainty in [O III]/[O II] vs. f_{esc}). The colored solid and dashed lines show the same for $8.0 < \log(M/M_\odot) < 8.5$ (brown), $8.5 < \log(M/M_\odot) < 9.0$ (beige), $9.0 < \log(M/M_\odot) < 9.5$ (green). **Right:** Comparison of our predicted $f_{esc}(z)$ to model reconstructions (Kuhlen & Faucher-Giguère 2012; Mitra et al. 2015; Price et al. 2016) and simulations (Sharma et al. 2016; Ma et al. 2015) from the literature. The color lines show the best fits to our predictions parametrized by $f_{esc}(z > 2) = f_{esc,0} \left((1+z)/3\right)^\alpha$ for $2 < z < 8$ (see Table 1).

8 detections of f_{esc} and 4 upper limits, each of them with reliable spectroscopic measurements of [O II] and [O III] (Leitet et al. 2013; Borthakur et al. 2014; Izotov et al. 2016a,b; Vanzella et al. 2016; Leitherer et al. 2016). The limit at [O III]/[O II] > 10 (estimated from only a spectroscopic detection of [O III]) and $f_{esc} > 50\%$ shows the recent detection at $z = 3.2$ (de Barros et al. 2016; Vanzella et al. 2016). The positive correlation between f_{esc} and [O III]/[O II] ratio is evident, although mostly driven by the limit at large f_{esc}. It should therefore be used with caution and its uncertainty must be included in the following analysis. We describe this relation with the analytical form

$$[\text{O III}]/[\text{O II}] = \phi + (\phi + a)^b + a, \qquad (1)$$

and use the substitution $\phi = \log(f_{esc})$. The best fit ($a = 2.60^{+0.09}_{-0.09}$ and $b = 2.52^{+0.83}_{-0.16}$) is shown as dashed line. The gray band shows the 1σ and 90% *asymmetric* confidence interval of the fit, which is determined by a bootstrapping method and takes into account the limits and uncertainties of the measurements. We will see that including the uncertainties of this relation lowers the predicted f_{esc} at a given redshift. The blue region in Figure 2 shows $f_{esc} > 10\%$, i.e., the value that must be reached by $z \sim 6$ such that galaxies can dominate reionization under the current knowledge. We see that these

values are reached at [O III]/[O II] $\sim 4 - 7$, corresponding to $z \gtrsim 6.5$ for average galaxies at $\log(M/M_\odot) \sim 9.0$ (Figure 1).

2.4. *Redshift evolution and mass dependence of f_{esc}*

Using the redshift evolution of [O III]/[O II] inferred from SDSS galaxies (left panel of Figure 1) and the empirical relation between [O III]/[O II] and f_{esc} (Equation 1, Figure 2), we can now predict f_{esc} as a function of redshift under the given uncertainties. For this end, we use a Monte-Carlo sampling approach taking into account the scatter in the [O III]/[O II] vs. redshift relation and the uncertainties/limits in the [O III]/[O II] vs. f_{esc} correlation. In detail, we sample 5000 galaxies for each redshift bin and draw [O III]/[O II] ratios to reproduce the observed distribution at a given redshift. For each of these galaxies we then draw f_{esc} from the corresponding [O III]/[O II] ratio, which distribution we approximate with a skewed gaussian to take into account its asymmetric uncertainties.

The left panel of Figure 3 shows the final distribution of $f_{esc}(z)$ for different stellar mass bins. The dashed lines *only* include the physical scatter in the [O III]/[O II] vs. redshift relation from our LHAs. The solid lines include the physical scatter *and* the uncertainty in the modeling of the [O III]/[O II] vs. f_{esc} relation. This in general

lowers the predicted $f_{\rm esc}$ values (indicated by the arrows) and better constraints on the correlation between [O III]/[O II] and $f_{\rm esc}$ are therefore crucial for a more detailed analysis. We also show the 1σ (90%) confidence interval of the prediction as dark (light) gray band for the stellar mass range $8.5 < \log(M/{\rm M}_\odot) < 9.5$ but omit it for the other masses for sake of clarity. Due to the $10 - 15\%$ higher [O III]/[O II] ratios for $\sim 0.5\,{\rm dex}$ lower stellar masses (see also Masters et al. 2016), $f_{\rm esc}$ shows a *negative* correlation with stellar mass. In general, $f_{\rm esc}$ is about 50% higher per $0.5\,{\rm dex}$ smaller stellar mass in the range $8.0 < \log(M/{\rm M}_\odot) < 9.5$ at $z \sim 6$. For the average population at $8.5 < \log(M/{\rm M}_\odot) < 9.5$, we find $f_{\rm esc} = 5.7^{+8.3}_{-3.3}\,\%$ at $z = 6$ and $f_{\rm esc} = 10.4^{+15.5}_{-6.3}\,\%$ at $z = 9$ (errors given as 1σ). Statistically, about 30% of the galaxies at $z \sim 6$ show $f_{\rm esc} > 10\%$, while this fraction becomes 50% at $z \sim 9$. We fit $f_{\rm esc} = f_{\rm esc,0}\,(1 + z)^\alpha$ for $2 < z < 8$ with $f_{\rm esc,0} = 2.3 \pm 0.1\,\%$ and $\alpha = 1.17 \pm 0.02$ in the same stellar mass range. The best fits for the different stellar mass bins in the same redshift bin are listed in Table 1. The left panel of Figure 3 compares our prediction of $f_{\rm esc}(z)$ with measurements in the literature from simulations (Ma et al. 2015; Sharma et al. 2016) or $f_{\rm esc}$ reconstructions from *Planck*, Lyman-α, and QSO data (Kuhlen & Faucher-Giguère 2012; Mitra et al. 2015; Price et al. 2016). In general, our predicted $f_{\rm esc}$ values are lower compared to other studies, except for the results from the *FIRE* simulation (Ma et al. 2015). It has to be kept in mind that there is a strong dependence of $f_{\rm esc}$ on stellar mass as described above, and our lowest stellar mass bin is consistent within 1σ with the literature.

Table 1. Fit to predicted $f_{\rm esc}(z)$ for different stellar mass bins.

stellar mass	$f_{\rm esc,0}$ [%]	α
$8.5 < \log(M/{\rm M}_\odot) < 9.5$	$1.7^{+0.1}_{-0.2}$	$1.37^{+0.11}_{-0.10}$
$8.0 < \log(M/{\rm M}_\odot) < 8.5$	$2.5^{+0.2}_{-0.2}$	$1.40^{+0.13}_{-0.10}$
$8.5 < \log(M/{\rm M}_\odot) < 9.0$	$2.1^{+0.2}_{-0.2}$	$1.26^{+0.11}_{-0.10}$
$9.0 < \log(M/{\rm M}_\odot) < 9.5$	$1.4^{+0.4}_{-0.3}$	$1.43^{+0.29}_{-0.41}$

Analytical expression: $f_{\rm esc}(z) = f_{\rm esc,0}\left((1 + z)/3\right)^\alpha$. The fit is performed between $2 < z < 8$.

3. CAN GALAXIES REIONIZE THE UNIVERSE?

We use the LHAs to predict $f_{\rm esc}(z)$ and find $\langle f_{\rm esc}\rangle \sim 6\%$ at $z = 6$ and $\langle f_{\rm esc}\rangle \sim 10\%$ at $z = 9$ for the stellar mass range $8.5 < \log(M/{\rm M}_\odot) < 9.5$. This prediction comes with a substantial physical scatter (due to the scatter in the [O III]/[O II] ratios at a given redshift) and uncertainty stemming from the poorly constrained [O III]/[O II] vs. $f_{\rm esc}$ relation. Statistically, $\sim 30\%$ of the galaxies show $f_{\rm esc} > 10\%$ by $z = 6$ for $8.5 < \log(M/{\rm M}_\odot) < 9.5$, however, there is a stellar mass dependence that increases $f_{\rm esc}$ by roughly 50% per $0.5\,{\rm dex}$ decrease in stellar mass (see Figure 3).

Is this enough for galaxies alone to reionize the universe? The recent study by Price et al. (2016) reconstructs $f_{\rm esc}(z)$ needed for reionization from the latest *Planck* data and finds $2 - 3$ times higher $f_{\rm esc}$ values at $z > 6$ compared to our predictions. Their findings are just consistent (within 1σ) with our observation based predictions for $f_{\rm esc}$ for the smallest stellar mass bin $(8.0 < \log(M/{\rm M}_\odot) < 8.5)$. This suggests that the commonly found galaxies at high redshifts with $\log(M/{\rm M}_\odot) \sim 9.0$ are not sufficient for ionizing the early universe, instead it is mostly driven by low-mass, low-luminosity galaxies at $\log(M/{\rm M}_\odot) \sim 8.0$.

In the following, we want to investigate the above question in more detail and derive two important quantities: $Q_{\rm HII}(z)$ (the volume fraction of ionized hydrogen) and $\tau_{\rm el}(z)$ (the integrated electron scattering optical depth). For this end, several assumption have to be made. First, the faint end cut off of the UV LF $(M_{\rm UV,lim})$ determines the number of faint galaxies that are available for ionization (similar to the stellar mass function, remember, $f_{\rm esc}$ is anti-correlated with stellar mass). High redshift galaxies lensed by foreground low redshift galaxy clusters allow us to probe the UV LF to very faint magnitudes of $M_{\rm UV} \sim -12$ at $z = 6 - 8$ and have shown no indication of a turn-over (Alavi et al. 2014; Livermore et al. 2016). It is therefore save to assume a value between $-13 < M_{\rm UV,lim} < -10$. Furthermore, the Lyman continuum photon production efficiency $(\xi_{\rm ion})$ and the clumping factor (C) need to be known. The former is measured observationally and is found to be $\log(\xi_{\rm ion}/[{\rm Hz\ erg}^{-1}]) = 25.4 \pm 0.1$ for a wide range of galaxy properties at $z \sim 5$ (Bouwens et al. 2015b). The clumping factor $C = \langle n_H^2\rangle/\bar{n}_H^2$ is proportional to the recombination rate of hydrogen[5] and thus the net production rate of ions. It is commonly constrained from simulations to be between 2 and 5, and we assume $\langle C\rangle = 3$ (e.g., Finlator et al. 2012). Other reasonable values of C have little impact on the following results.

With the relatively good constraints on $\xi_{\rm ion}$ and C and our empirical prediction of $f_{\rm esc}(z)$ we can now derive $Q_{\rm HII}(z)$ and $\tau_{\rm el}(z)$ using the following set of basic equations.

---

[5] The recombination rate is proportional to the hydrogen density squared.
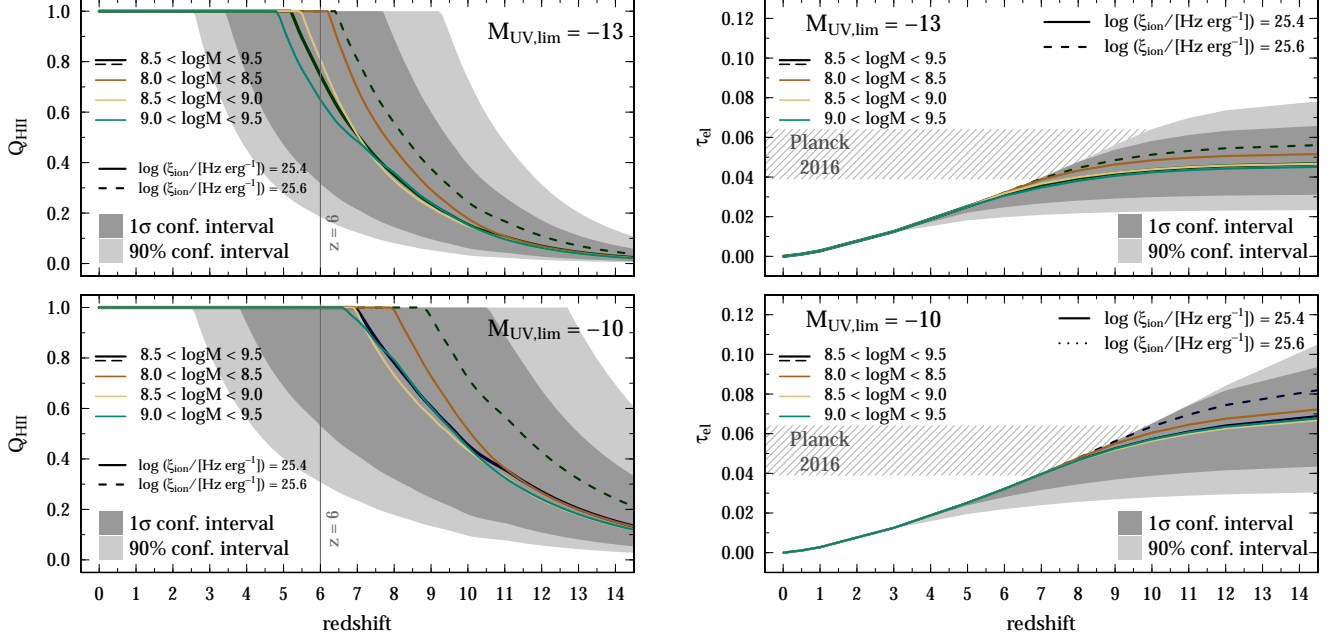
Figure 4. **Left:** Volume fraction of ionized hydrogen as a function of redshift assuming $\log(\xi_{\rm ion}) = 25.4$ for $M_{\rm UV,lim} = -13$ (top) and $M_{\rm UV,lim} = -10$ (bottom) with 1σ and 90% confidence intervals (for $8.5 < \log(M/{\rm M_\odot}) < 9.5$, only). The different stellar mass bins are indicated with colors. The thin line marks $z < 6$ when the universe is observed to be fully ionized. We also show $\log(\xi_{\rm ion}) = 25.6$ for $8.5 < \log(M/{\rm M_\odot}) < 9.5$ as dashed line for reference. **Right:** Electron scattering optical depth integrated up to different redshifts for $M_{\rm UV,lim} = -13$ (top) and $M_{\rm UV,lim} = -10$ (bottom) with 1σ and 90% confidence intervals (for $8.5 < \log(M/{\rm M_\odot}) < 9.5$, only). The different stellar mass bins are indicated with colors. The gray hatched band marks the recent constraints from *Planck*. We also show $\log(\xi_{\rm ion}) = 25.6$ for $8.5 < \log(M/{\rm M_\odot}) < 9.5$ as dashed line. All in all, we find that our observational based prediction of $f_{\rm esc}$ are just enough for galaxies to reionize the universe by $z \sim 5.3$. Lower mass galaxies are predicted to reionize the universe by $\Delta z \sim 0.5$ earlier.

$$\tau_{\rm el}(z) = c \langle n_{\rm H} \rangle \sigma_{\rm T} \int_0^z f_{\rm e} Q_{\rm HII}(z') H^{-1}(z')(1+z')^2 dz' \quad (2)$$

$$\dot{Q}_{\rm HII} = \frac{\dot{n}_{\rm ion}}{\langle n_{\rm H} \rangle} - \frac{Q_{\rm HII}}{t_{\rm rec}} \quad (3)$$

$$\dot{n}_{\rm ion} = f_{\rm esc} \xi_{\rm ion} \rho_{\rm uv} \quad (4)$$

$$t_{\rm rec} = \left[C \, \alpha_B(T)(1 + Y_p/4X_p) \langle n_{\rm H} \rangle (1+z)^3 \right]^{-1} \quad (5)$$

$$\alpha_B = 2.6 \times 10^{-13} \left(\frac{T}{10^4 {\rm K}} \right)^{-0.76} {\rm cm^3/s} \quad (6)$$

$$\langle n_H \rangle = 1.67 \times 10^{-7} \left(\frac{\Omega_b h^2}{0.02} \right) \left(\frac{X_p}{0.75} \right) {\rm cm^{-3}} \quad (7)$$

where t_{rec} is the hydrogen recombination time with α_B the case B recombination coefficient. We assume $X_p = 0.75$ for the hydrogen mass fraction (e.g., Hou et al. 2011), the helium mass fraction is given as $Y_p = 1 - X_p$ (Kuhlen & Faucher-Giguère 2012), and a fraction of free electrons as $f_e = 1 + Y_p/2X_p$ at $z \leq 4$

and $f_e = 1 + Y_p/4X_p$ at $z > 4$. Furthermore, we use a baryon density $\Omega_b = 0.04$, the Thompson scattering cross-section $\sigma_{\rm T} = 6.653 \times 10^{-25} \, {\rm cm^2}$, and an IGM temperature $T = 20,000 \, {\rm K}$. We assume $C = 3$ and $\log(\xi_{\rm ion}) = 25.4$ and 25.6. For the integrated UV luminosity density, $\rho_{\rm uv}$, we use $M_{\rm UV,lim} = -13$ and -10 and the UV luminosity functions by Mason et al. (2015).

With our observationally driven prediction of $f_{\rm esc}(z)$ and our reasonable assumptions for C and $\xi_{\rm ion}$, we can now investigate whether galaxies can reionize the universe by $z \sim 6$. The left panels of Figure 4 show $Q_{\rm HII}(z)$ for $M_{\rm UV,lim} = -13$ (top) and -10 (bottom). The 1σ and 90% confidence intervals from our $f_{\rm esc}$ predictions are given for $\log(\xi_{\rm ion}) = 25.4$ and $8.5 < \log(M/{\rm M_\odot}) < 9.5$. We also show $\log(\xi_{\rm ion}) = 25.6$ as dashed line for reference. The population averaged ($8.5 < \log(M/{\rm M_\odot}) < 9.5$) results are shown in black together with other stellar mass bins with colors as in Figure 3. The right panels of Figure 4 show $\tau_{\rm el}(z)$ with the same color coding and assumptions. We find that, galaxies with $\log(M/{\rm M_\odot}) \sim 9.0$ are capable of ionizing the IGM by $z_{\rm ion} = 5.3^{-1.8}_{+2.4}$ and yield $\tau_{\rm el} \sim 0.05$ with the combination $(M_{\rm UV,lim}, \log \xi_{\rm ion}) = (-13, 25.4)$. Note that this is a population averaged quantity and single galaxies may show very different escape fractions

and therefore contribute to a non-isotropic reionization of the universe. Particularly, due to the negative correlation between [O III]/[O II] and stellar mass, a population of low mass galaxies ($\log(M/\mathrm{M}_\odot) \sim 8.0 - 8.5$) will reionize the universe slightly earlier ($\Delta z \sim 0.5$, so roughly at $z \sim 6$). These findings are in good agreement with measurement of Lyα forest transmission, quasar absorption, and gamma-ray bursts (e.g., Fan et al. 2006; Totani et al. 2006; Bolton & Haehnelt 2007a; McQuinn et al. 2008; Faucher-Giguère et al. 2008; Carilli et al. 2010; Bolton et al. 2011; McGreer et al. 2011; Mortlock et al. 2011; Schroeder et al. 2013) as well as the constraint from *Planck* on the electron scattering optical depth (upper right panel of Figure 4). The combination $(M_{\mathrm{UV,lim}}, \log \xi_{\mathrm{ion}}) = (-10, 25.4)$ yields $z_{\mathrm{ion}} = 6.9^{-3.1}_{+3.5}$, which is also in agreement within uncertainties with the complementary observational constraints, but it overshoots the constraints on τ_{el} by *Planck*; it leads to a too early reionization. This analysis also depends on the assumed value for ξ_{ion} (see dashed line in Figure 4 showing $\log(\xi_{\mathrm{ion}}) = 25.6$) and in particular higher ξ_{ion} have the same effect as lowering stellar mass and lead to an earlier reionization. There are not much constraints on the dependency of ξ_{ion} on other galaxy properties. However, Bouwens et al. (2015b) see a weak *negative* trend between the UV continuum slope (β) and ξ_{ion} in their data at $3.8 < z < 5.0$. Assuming a *positive* correlation between stellar mass and β (i.e., more massive galaxies having shallower slopes and likely more dust, e.g., Finkelstein et al. 2012; Bouwens et al. 2014), this would suggest a *smaller* ξ_{ion} for more massive galaxies. These trends thus suggest that less massive galaxies might be even more efficient in ionizing, or, vice versa, more massive galaxies less.

4. CONCLUSIONS

We use empirical trends seen in local galaxies to predict emission line ratios and Lyman continuum escape fractions at high redshifts. For this end, we combine the positive correlation of the [O III]/[O II] line ratio and f_{esc} based on low redshift galaxies with the predicted [O III]/[O II] ratios at high redshift from LHAs. We find increasing [O III]/[O II] line ratios with increasing redshifts reaching values of [O III]/[O II] $\sim 3 - 4$ commonly by $z = 6$, which translates into $f_{\mathrm{esc}} > 6\%$ on average

at $z > 6$ for galaxies with $\log(M/\mathrm{M}_\odot) \sim 9.0$. Statistically, including uncertainties and scatter, roughly 30% of galaxies at $z = 6$ show $f_{\mathrm{esc}} > 10\%$ and this fraction increases to 50% at $z = 9$. This first observation based prediction of f_{esc} suggests that its values for high redshift galaxies are substantially higher than the currently low f_{esc} limits measured in low-z galaxies and thus hints towards a strong redshift evolution of f_{esc}. However, we also find a strong stellar mass dependency of f_{esc}, driven by the stellar mass dependency of the [O III]/[O II] ratio. In particular, a decrease by 0.5 dex in stellar mass results in an *increase* in f_{esc} of 50%. Note that this is in agreement with the dark matter halo dependency of f_{esc} predicted by various simulations. If true, the stellar mass function and its evolution with redshift – that is likely coupled with the rest-UV luminosity function – is an important ingredient to access the importance of galaxies in the EoR. With our observation based prediction for the population averaged $f_{\mathrm{esc}}(z)$ (thus fixing an important previously unknown variable) and reasonable assumptions for C and ξ_{ion} we find that galaxies at $\log(M/\mathrm{M}_\odot) \sim 9.0$ release a sufficiently large number of ionizing photons to reionize the universe by $z_{\mathrm{ion}} = 5.3^{-1.8}_{+2.4}$ for $M_{\mathrm{UV,lim}} = -13$ and $z_{\mathrm{ion}} = 6.9^{-3.1}_{+3.5}$ for $M_{\mathrm{UV,lim}} = -10$. Galaxies at lower masses are able to reionize the universe by $\Delta z \sim 0.5$ earlier.

This work should be understood as the beginning of a more detailed study of f_{esc} during the EoR. Until now, it is still hampered by the large uncertainties in the [O III]/[O II] vs. f_{esc} relation. Furthermore, the link between LHA and actual very high redshift galaxies needs to be explored in more detail. Future spectroscopic observations by the *Hubble Space Telescope* will enhance the sample sizes of galaxies with LyC detection and will add to a better understanding of the link between [O III]/[O II] and f_{esc}. Furthermore, *WFIRST* and *JWST* will ultimately measure [O III] and [O II] in high redshift galaxies and thus verify the link between local galaxies and the first galaxies formed.

REFERENCES

Alam, S., Albareti, F. D., Allende Prieto, C., et al. 2015, ApJS, 219, 12

Alavi, A., Siana, B., Richard, J., et al. 2014, ApJ, 780, 143

Bian, F., Kewley, L. J., Dopita, M. A., & Juneau, S. 2016, ApJ, 822, 62

Bolton, J. S., & Haehnelt, M. G. 2007a, MNRAS, 381, L35

—. 2007b, MNRAS, 382, 325

Bolton, J. S., Haehnelt, M. G., Warren, S. J., et al. 2011, MNRAS, 416, L70

Borthakur, S., Heckman, T. M., Leitherer, C., & Overzier, R. A. 2014, Science, 346, 216

Bouwens, R. J., Illingworth, G. D., Oesch, P. A., et al. 2015a, ApJ, 811, 140

Bouwens, R. J., Smit, R., Labbe, I., et al. 2015b, ArXiv e-prints, arXiv:1511.08504

Bouwens, R. J., Illingworth, G. D., Oesch, P. A., et al. 2014, ApJ, 793, 115

—. 2015c, ApJ, 803, 34

Cardamone, C., Schawinski, K., Sarzi, M., et al. 2009, MNRAS, 399, 1191

Carilli, C. L., Wang, R., Fan, X., et al. 2010, ApJ, 714, 834

Chabrier, G. 2003, PASP, 115, 763

Colbert, J. W., Teplitz, H., Atek, H., et al. 2013, ApJ, 779, 34

Cooke, J., Ryan-Weber, E. V., Garel, T., & Díaz, C. G. 2014, MNRAS, 441, 837

de Barros, S., Vanzella, E., Amorín, R., et al. 2016, A&A, 585, A51

de los Reyes, M. A., Ly, C., Lee, J. C., et al. 2015, AJ, 149, 79

Erb, D. K., Pettini, M., Steidel, C. C., et al. 2016, ArXiv e-prints, arXiv:1605.04919

Faisst, A. L., Capak, P., Carollo, C. M., Scarlata, C., & Scoville, N. 2014, ApJ, 788, 87

Faisst, A. L., Capak, P., Hsieh, B. C., et al. 2016a, ApJ, 821, 122

Faisst, A. L., Capak, P. L., Davidzon, I., et al. 2016b, ApJ, 822, 29

Fan, X., Strauss, M. A., Becker, R. H., et al. 2006, AJ, 132, 117

Faucher-Giguère, C.-A., Prochaska, J. X., Lidz, A., Hernquist, L., & Zaldarriaga, M. 2008, ApJ, 681, 831

Finkelstein, S. L., Papovich, C., Salmon, B., et al. 2012, ApJ, 756, 164

Finlator, K., Oh, S. P., Özel, F., & Davé, R. 2012, MNRAS, 427, 2464

Förster Schreiber, N. M., Shapley, A. E., Erb, D. K., et al. 2011, ApJ, 731, 65

Gnedin, N. Y., Kravtsov, A. V., & Chen, H.-W. 2008, ApJ, 672, 765

Grazian, A., Giallongo, E., Gerbasi, R., et al. 2016, A&A, 585, A48

Greis, S. M. L., Stanway, E. R., Davies, L. J. M., & Levan, A. J. 2016, MNRAS, 459, 2591

Guaita, L., Pentericci, L., Grazian, A., et al. 2016, A&A, 587, A133

Hayashi, M., Ly, C., Shimasaku, K., et al. 2015, PASJ, 67, 80

Hemmati, S., Mobasher, B., Darvish, B., et al. 2015, ApJ, 814, 46

Hou, L. G., Han, J. L., Kong, M. Z., & Wu, X.-B. 2011, ApJ, 732, 72

Hu, E. M., Cowie, L. L., Kakazu, Y., & Barger, A. J. 2009, ApJ, 698, 2014

Inoue, A. K., Iwata, I., & Deharveng, J.-M. 2006, MNRAS, 371, L1

Inoue, A. K., Shimizu, I., Iwata, I., & Tanaka, M. 2014, MNRAS, 442, 1805

Izotov, Y. I., Orlitová, I., Schaerer, D., et al. 2016a, Nature, 529, 178

Izotov, Y. I., Schaerer, D., Thuan, T. X., et al. 2016b, ArXiv e-prints, arXiv:1605.05160

Khostovan, A. A., Sobral, D., Mobasher, B., et al. 2016, ArXiv e-prints, arXiv:1604.02456

Kuhlen, M., & Faucher-Giguère, C.-A. 2012, MNRAS, 423, 862

Le Fèvre, O., Cassata, P., Cucciati, O., et al. 2013, A&A, 559, A14

Leitet, E., Bergvall, N., Hayes, M., Linné, S., & Zackrisson, E. 2013, A&A, 553, A106

Leitherer, C., Hernandez, S., Lee, J. C., & Oey, M. S. 2016, ArXiv e-prints, arXiv:1603.06779

Livermore, R. C., Finkelstein, S. L., & Lotz, J. M. 2016, ArXiv e-prints, arXiv:1604.06799

Ma, X., Kasen, D., Hopkins, P. F., et al. 2015, MNRAS, 453, 960

Madau, P. 1995, ApJ, 441, 18

Madau, P., & Haardt, F. 2015, ApJL, 813, L8

Maiolino, R., Nagao, T., Grazian, A., et al. 2008, A&A, 488, 463

Mason, C. A., Trenti, M., & Treu, T. 2015, ApJ, 813, 21

Masters, D., Faisst, A., & Capak, P. 2016, ArXiv e-prints, arXiv:1605.04314

Masters, D., Capak, P., Salvato, M., et al. 2012, ApJ, 755, 169

Matthee, J. J. A., Sobral, D., Swinbank, A. M., et al. 2014, MNRAS, 440, 2375

McGreer, I. D., Mesinger, A., & Fan, X. 2011, MNRAS, 415, 3237

McQuinn, M., Lidz, A., Zaldarriaga, M., Hernquist, L., & Dutta, S. 2008, MNRAS, 388, 1101

Mitra, S., Choudhury, T. R., & Ferrara, A. 2015, MNRAS, 454, L76

Mortlock, D. J., Warren, S. J., Venemans, B. P., et al. 2011, Nature, 474, 616

Nakajima, K., & Ouchi, M. 2014, MNRAS, 442, 900

Oesch, P. A., Bouwens, R. J., Illingworth, G. D., et al. 2014, ApJ, 786, 108

Ono, Y., Ouchi, M., Mobasher, B., et al. 2012, ApJ, 744, 83

Palanque-Delabrouille, N., Magneville, C., Yèche, C., et al. 2013, A&A, 551, A29

Planck Collaboration, Aghanim, N., Ashdown, M., et al. 2016, ArXiv e-prints, arXiv:1605.02985

Price, L. C., Trac, H., & Cen, R. 2016, ArXiv e-prints, arXiv:1605.03970

Razoumov, A. O., & Sommer-Larsen, J. 2010, ApJ, 710, 1239

Rigby, J. R., Wuyts, E., Gladders, M. D., Sharon, K., & Becker, G. D. 2011, ApJ, 732, 59

Roberts-Borsani, G. W., Bouwens, R. J., Oesch, P. A., et al. 2015, ArXiv e-prints, arXiv:1506.00854

Robertson, B. E., Ellis, R. S., Furlanetto, S. R., & Dunlop, J. S. 2015, ApJL, 802, L19

Rutkowski, M. J., Scarlata, C., Haardt, F., et al. 2016, ApJ, 819, 81

Sandberg, A., Östlin, G., Melinder, J., Bik, A., & Guaita, L. 2015, ApJL, 814, L10

Sanders, R. L., Shapley, A. E., Kriek, M., et al. 2016, ApJ, 816, 23

Schenker, M. A., Robertson, B. E., Ellis, R. S., et al. 2013, ApJ, 768, 196

Schroeder, J., Mesinger, A., & Haiman, Z. 2013, MNRAS, 428, 3058

Sharma, M., Theuns, T., Frenk, C., et al. 2016, MNRAS, 458, L94

Siana, B., Shapley, A. E., Kulas, K. R., et al. 2015, ApJ, 804, 17

Silverman, J. D., Kashino, D., Sanders, D., et al. 2015, ApJS, 220, 12

Smith, B. M., Windhorst, R. A., Jansen, R. A., et al. 2016, ArXiv e-prints, arXiv:1602.01555

Stanway, E. R., Eldridge, J. J., Greis, S. M. L., et al. 2014, MNRAS, 444, 3466

Stark, D. P., Ellis, R. S., Chiu, K., Ouchi, M., & Bunker, A. 2010, MNRAS, 408, 1628

Steidel, C. C., Pettini, M., & Adelberger, K. L. 2001, ApJ, 546, 665

Steidel, C. C., Rudie, G. C., Strom, A. L., et al. 2014, ApJ, 795, 165

Tacchella, S., Trenti, M., & Carollo, C. M. 2013, ApJL, 768, L37

Totani, T., Kawai, N., Kosugi, G., et al. 2006, PASJ, 58, 485

Vanzella, E., de Barros, S., Vasei, K., et al. 2016, ArXiv e-prints, arXiv:1602.00688

Vasei, K., Siana, B., Shapley, A. E., et al. 2016, ArXiv e-prints, arXiv:1603.02309

Wise, J. H., & Cen, R. 2009, ApJ, 693, 984

York, D. G., Adelman, J., Anderson, Jr., J. E., et al. 2000, AJ,
120, 1579